

## Predictive simulations of impurity transport at JET

D. Tegner<sup>1</sup>, P. Strand<sup>1</sup>, H. Nordman<sup>1</sup>, L. Fazendeiro<sup>1</sup>, A. Skyman<sup>1</sup>, P. Belo<sup>2</sup>, C. Giroud<sup>3</sup>,  
and the JET-EFDA Contributors.\*

JET-EFDA, Culham Science Centre, OX14 3DB, Abingdon, UK.

<sup>1</sup> *Department of Earth and Space Sciences, Chalmers University of Technology, Euratom-VR Association, SE-412 96 Göteborg, Sweden.*

<sup>2</sup> *Associação EURATOM-IST, Instituto de Plasmas e Fusão Nuclear, Instituto Superior Técnico, Av Rovisco Pais, 1049-001 Lisbon, Portugal.*

<sup>3</sup> *EURATOM/CCFE Association, Culham Science Centre, Abingdon, OX14 3DB UK.*

\* *See the Appendix of F. Romanelli et al., Proceedings of the 24th IAEA Fusion Energy Conference 2012, San Diego, US*

### Introduction

In the present study, the impact of sheared toroidal rotation on L-mode and H-mode experiments with carbon wall at the Joint European Torus are analysed using the coupling between the transport codes JETTO<sup>1</sup> (for main ions) and SANCO (for impurities) for predictive simulations. Transport coefficients due to Ion-Temperature-Gradient (ITG) mode and Trapped-Electron (TE) mode turbulence are used together with neoclassical transport from NCLASS. The transport coefficients obtained using the Chalmers fluid model,<sup>2</sup> updated with the roto-diffusion associated with sheared rotation, are compared with gyrokinetic results using the code GENE.<sup>3</sup> Self-consistent simulations of electron and ion temperatures, main ion and impurity densities are performed while the toroidal momentum profile is treated interpretatively. The role of neoclassical impurity transport is evaluated and the dependence of the simulated profiles on impurity charge number  $Z$ , rotation gradient (roto-diffusion), and impurity charge fraction ( $Z_{\text{eff}}$ ) are discussed. In particular the impact of sheared toroidal rotation on the C profiles is investigated. The considered discharges include L-mode impurity injection experiment #67730, as well as a H-mode discharge. The impurity behaviour in the L-mode and H-mode discharges are compared, however, experimental data for the impurity transport coefficients are only available for the L-mode discharge.<sup>4</sup>

## Transport models

The Weiland multi-fluid model,<sup>2</sup> updated with effects of sheared rotation (roto-diffusion)<sup>5</sup> on the impurity transport coefficients, has been used in the predictive simulations to describe the ITG/TE mode turbulence and the impurity species. The impurity flux is calculated as  $\Gamma_Z = \langle v_{\text{ExB}} \delta n_Z \rangle = -D_Z \nabla n_Z + n_Z V_Z$  where  $D_Z$  is the diffusivity and  $V_Z$  is the convective velocity, including contributions from thermodiffusion, curvature, parallel compression, and roto-diffusion. In steady state the zero impurity flux condition  $\Gamma_Z = 0$  gives the impurity density normalized inverse scale length  $\text{PF} = -R \nabla n_Z / n_Z = -R V_Z / D_Z$  from the balance between the outward diffusion and convection, giving  $\text{PF} > 0$  for inward convective velocity and  $\text{PF} < 0$  for  $V_Z > 0$ .

The kinetic results have been obtained with the gyrokinetic code GENE.<sup>3</sup> The QL GENE simulations calculate the flux from the dominant mode, which is the ITG mode for the discharges considered.

## Roto-diffusion

The effects of sheared rotation in the form of roto-diffusion on the impurity density normalized inverse scale length  $\text{PF} = -R V_Z / D_Z$  are calculated for the considered discharges using the fluid model which is benchmarked against quasi-linear gyrokinetic simulations. The simulations have been performed in a simple  $s$ - $\alpha$  equilibrium in the electrostatic limit. In a previous interpretative study of the L-mode impurity injection discharge #67730, neglecting roto-diffusion, it was showed that the predicted values of  $D_Z$  and  $V_Z$  and the  $Z$ -scaling were in reasonable agreement with experimental values.<sup>6</sup> For Carbon however, the predicted impurity density normalized inverse scale length was significantly larger than indicated by the measured C profile which is flat or hollow at mid-radius.

The scaling of the impurity density normalized inverse scale length with shearing rate  $\gamma_{\text{ExB}}$  for #67730 are displayed in Fig. 1. As observed, the fluid and GENE results are in good agreement and show that impurity density normalized inverse scale lengths are reduced by the shearing rate leading to a reversal of the impurity pinch, from inward ( $\text{PF} > 0$ ) to outward ( $\text{PF} < 0$ ), for  $\gamma_{\text{ExB}} \geq 0.23$  for Carbon. This effect was found to be crucial for the explanation of the hollow Boron profiles in ASDEX-U.<sup>7</sup> In the present case, however, the shearing rate is too small (indicated by the vertical dashed line in Fig. 1) to explain the flat or hollow C profile observed in the JET experiment.

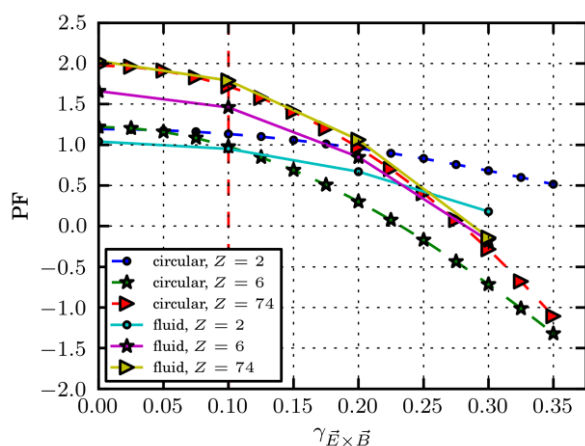


**Fig. 1.** Effects of shear in toroidal flow on impurity density normalized inverse scale lengths ( $-R\nabla n_z/n_z$ ), including contributions from roto-diffusion ( $\frac{dv_{\parallel}}{dr}$  - pinch). The perpendicular and parallel flow shear is controlled by the parameter  $\gamma_{ExB} = -\frac{r/R}{q_0} \frac{\partial \Omega}{\partial x} \frac{R}{c_s}$ . Results obtained by fluid and quasi-linear GENE simulations of #67730 in the collisionless, electrostatic limit.

### Predictive simulations

In order to complement the interpretative study,<sup>6</sup> predictive simulations of  $T_i$ ,  $T_e$ ,  $n_e$  and  $n_z$  profiles (one impurity species) are performed, with the toroidal rotation treated interpretatively, using the coupling between the transport codes JETTO and SANCO. SANCO solves continuity equations for all ionization stages using neoclassical transport and ITG/TE mode impurity transport from JETTO, here using the standard Weiland interface. Impurity profiles are obtained for impurities varying from He ( $Z=2$ ) to Ni ( $Z=28$ ). In the numerical simulations the SANCO settings use a radially constant  $Z_{\text{eff}}$  profile as initial condition without impurity gas puffing, with no losses in the SOL and with a recycling coefficient equal to one. Trace levels of impurities are used as initial conditions as well as larger levels like the experimentally relevant situation with 2% C for comparison. In the simulations, the separatrix boundary conditions for main ion density and temperature are adjusted so that the boundary values at  $\rho=r/a=0.9$  agree with the experimental values. For discharge #67730, the steady state profiles of  $T_i$ ,  $T_e$ , and  $n_e$ , obtained after 2 seconds of simulation time, are compared with the experimental profiles in Fig. 2a. The corresponding steady state profiles ( $R/L_{nz}$ ) of low to medium  $Z$  impurities with  $Z=2$ ,  $Z=4$ ,  $Z=6$ ,  $Z=10$ ,  $Z=18$  and  $Z=28$  are shown in Fig. 2b. As observed, the increase in impurity density normalized inverse scale length occurs mainly in the inner and outer core region where neoclassical effects dominate. At mid radius, turbulent transport dominates and the self-consistent impurity impurity density normalized inverse scale lengths are in reasonable agreement with the interpretative analysis.<sup>6</sup> Simulations including ExB shearing (interpretatively) and 2% background Carbon show that these effects only have a marginal effect on the Carbon density profile shape.

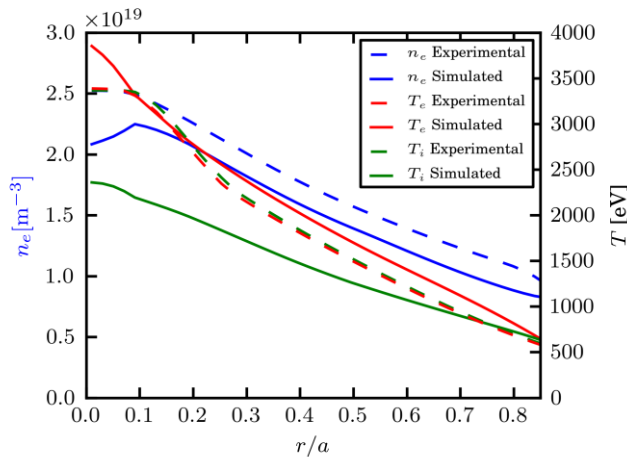


**Fig. 2a.** Steady state experimental and simulated profiles of  $T_i$ ,  $T_e$ , and  $n_e$  after 2.0 s of simulation time, shot #67730.

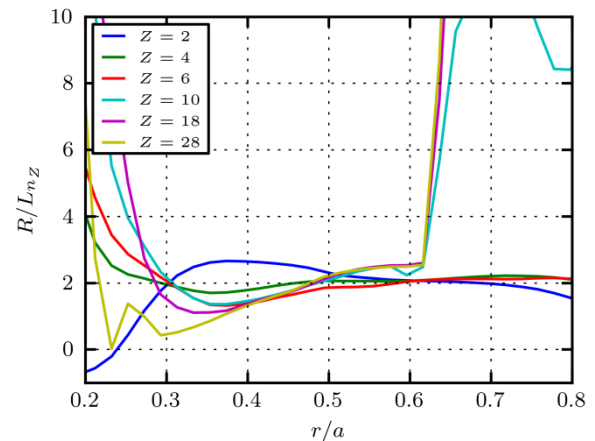


**Fig. 2b.** Impurity density normalized inverse scale lengths, shot #67730.

## Acknowledgements

*This work was supported by EURATOM and carried out within the framework of the European Fusion Development Agreement. The views and opinions expressed herein do not necessarily reflect those of the European Commission.*

## References

1. G. Cennachi and A. Taroni, JETTO: Tech. Rep. JET-IR(88)03 JET Reports (1988).
2. J. Weiland, Collective Modes in Inhomogeneous Plasmas, IoP (2000).
3. F. Jenko et al., Physics of Plasmas 7, 1904 (2000).
4. C. Giroud, C. Angioni, L. Carraro, et al, Proceedings of 34th EPS Conference on Controlled Fusion and Plasma Physics, Warszawa, Vol. 31 F, P-2.049 (2007).
5. Y. Camenen, A. G. Peeters, C. Angioni, F. J. Casson, W. A. Hornsby, A. P. Snodin, and D. Strintzi, Phys. Plasmas 16, 012503 (2009).
6. Nordman H, Skyman A, Strand P, Giroud C, Jenko F, Merz F, Naulin V, Tala T and the JET–EFDA contributors, Plasma Phys. Contr. F. 53 105005 (2011).
7. Angioni C, McDermott R, Fable E, Fischer R, Pütterich T, Rytter F, Tardini G and the ASDEX Upgrade Team, Nucl. Fusion 51, 023006 (2011).